Article:
Lorente Pons, A., Higginbottom, A. orcid.org/0000-0002-3246-6695, Cooper-Knock, J. et al. (6 more authors) (2020) Oligodendrocyte pathology exceeds axonal pathology in white matter in human amyotrophic lateral sclerosis. The Journal of Pathology, 251 (3). pp. 262-271. ISSN 0022-3417

https://doi.org/10.1002/path.5455

Journal of Pathology
J Pathol 2020; **00:** 000–000
Published online 00 Month 0000 in Wiley Online Library (wileyonlinelibrary.com) DOI: 10.1002/path.5455

ORIGINAL PAPER

Oligodendrocyte pathology exceeds axonal pathology in white matter in human amyotrophic lateral sclerosis

Alejandro Lorente Pons[1,2], Adrian Higginbottom[1], Johnathan Cooper-Knock[1], Aziza Alrafiah[1,3], Ebtisam Alofi[1,4], Janine Kirby[1], Pamela J Shaw[1], Jonathan D Wood[1] and J Robin Highley[1]*

[1] *Sheffield Institute for Translational Neuroscience, University of Sheffield, Sheffield, UK*
[2] *School of Biochemistry, University of Bristol, Bristol, UK*
[3] *Medical Laboratory Technology Department, Faculty of Applied Medical Sciences, Medical School, King AbdulAziz University, Jeddah, Saudi Arabia*
[4] *Department of Physiology, Faculty of Medicine, Medical School, King AbdulAziz University, Jeddah, Saudi Arabia*

**Correspondence to: JR Highley, Sheffield Institute for Translational Neuroscience, University of Sheffield, 385A Glossop Road, Sheffield, S10 2HQ, UK. E-mail: robin.highley@sheffield.ac.uk*

Abstract

Amyotrophic lateral sclerosis (ALS) is a neurodegenerative disease. The majority of cases are sporadic (sALS), while the most common inherited form is due to *C9orf72* mutation (C9ALS). A high burden of inclusion pathology is seen in glia (including oligodendrocytes) in ALS, especially in C9ALS. *Myelin basic protein* (*MBP*) messenger RNA (mRNA) must be transported to oligodendrocyte processes for myelination, a possible vulnerability for normal function. TDP43 is found in pathological inclusions in ALS and is a component of mRNA transport granules. Thus, TDP43 aggregation could lead to MBP loss. Additionally, the hexanucleotide expansion of mutant C9ALS binds hnRNPA2/B1, a protein essential for mRNA transport, causing potential further impairment of hnRNPA2/B1 function, and thus myelination. Using immunohistochemistry for p62 and TDP43 in human post-mortem tissue, we found a high burden of glial inclusions in the prefrontal cortex, precentral gyrus, and spinal cord in ALS, which was greater in C9ALS than in sALS cases. Double staining demonstrated that the majority of these inclusions were in oligodendrocytes. Using immunoblotting, we demonstrated reduced MBP protein levels relative to PLP (a myelin component that relies on protein not mRNA transport) and neurofilament protein (an axonal marker) in the spinal cord. This MBP loss was disproportionate to the level of PLP and axonal loss, suggesting that impaired mRNA transport may be partly responsible. Finally, we show that in C9ALS cases, the level of oligodendroglial inclusions correlates inversely with levels of hnRNPA2/B1 and the number of oligodendrocyte precursor cells. We conclude that there is considerable oligodendrocyte pathology in ALS, which at least partially reflects impairment of mRNA transport.

Keywords: amyotrophic lateral sclerosis; motor neurone disease; oligodendrocyte; myelin; axon; post-mortem RNA transport

Received 6 December 2019; Revised 11 April 2020; Accepted 27 April 2020

No conflicts of interest were declared.

Introduction

Amyotrophic lateral sclerosis (ALS) is a fatal, adult-onset, degenerative motor neurone disease with an incidence of ~1.5–2 per 100 000 people per year [1,2]. About 95% of cases are sporadic (sALS), while 5% are familial (fALS) [3]. An increasing number of gene mutations have been associated with ALS, the most frequent being *SOD1*, *TARDBP*, *FUS*, and *C9orf72*. The condition is characterised by both upper and lower motor neurone clinical features [2] and a pathological picture of upper and lower motor neurone and axon degradation, often with other, extra motor, brain areas involved. A subset of residual cells in affected regions accumulate pathological cytoplasmic inclusions of hyperphosphorylated, transactive response DNA-binding protein 43 kDa (TDP43) that is normally involved in multiple aspects of RNA processing [4,5]. These inclusions may also be immunolabelled with antisera for ubiquitin and p62. While TDP43 is normally present in the nucleus, in cells with inclusions, the nucleus is depleted of TDP43. This so-called TDP43 proteinopathy is most commonly considered in the context of neuronal pathology. However, it is established that TDP43 inclusions are seen in glia [4,6], and there is significant interest in an important role for glia in the pathogenesis of ALS. This has led to study of the trophic support that glia give to motor neurones and how this is affected by ALS [4,7,8]. For example, it has recently been demonstrated that oligodendrocytes derived from ALS cases can induce motor neurone death in co-culture [9].

Chromosome 9 open reading frame 72 (*C9orf72*) is the most commonly mutated gene in ALS, accounting

for around 37.6% of fALS cases (C9ALS) [10]. Mutations take the form of an expanded GGGGCC hexanucleotide repeat in intron 1 [11,12]. C9ALS cases show the classical pathology of motor neurone loss and TDP43 proteinopathy (with a high burden of glial inclusions). However, in addition, RAN-translated dipeptide repeats (DPRs) form cytoplasmic and intra-nuclear neuronal inclusions which are negative for TDP43. These are largely seen in the forebrain and cerebellum [13].

Oligodendrocytes are glia responsible for forming myelin sheaths, which act as electrical insulators and support axonal homeostasis [14]. Myelination involves oligodendrocyte processes wrapping axons with multiple membrane layers. This assembly is triggered by a phase transition of myelin basic protein (MBP), from a soluble to a more viscous form [15]. MBP is not translated in the cell body, where it would cause a fatal compaction of the organelle membranes. Instead, *MBP* mRNA is silenced and transported to the myelin compartment by the RNA transport granule, a complex of proteins and RNA molecules. For transport to occur, the *MBP* mRNA must be appropriately spliced and contain the so-called A2 response element (A2RE) in the 3′ UTR. The A2RE binds hnRNPA2/B1, which triggers the assembly of the mRNA-transport granule. Translation then occurs in the myelin compartment [16].

There are a number of reasons to suppose that disruptions to this process may be relevant to *C9orf72*-ALS and ALS more broadly. Firstly, *C9orf72* binds hnRNPA2/B1 and mediates its shuttling between the nucleus and cytoplasm [17]. Secondly, TDP43 is a component of the transport granule [18]. Therefore, it is possible that the pathological aggregation of TDP43 could impair mRNA transport and thus the delivery of *MBP* mRNA to the myelin compartment, resulting in impaired formation. In support of this, it appears that oligodendrocyte-specific deletion of TDP43 results in defective myelination in mice [19].

It has long been established that there is myelin loss in the motor system in ALS [20]. Interest is still current: In human post-mortem material, a recent analysis using a combination of methods (magnetic resonance diffusion and polarised light imaging and immunohistochemistry) found reduced myelin integrity in the perforant pathway [21]. A further study found degeneration of oligodendrocytes and myelin deficits in the SOD1 mouse model of ALS and foci of grey matter myelin loss in human post-mortem motor cortex [22]. Interestingly, radiological evidence is emerging to suggest that myelin degradation may precede axonal changes in neurodegenerative disease [23]. Traditionally, it has been assumed that at least some of this is secondary to axonal loss. However, it remains possible that oligodendrocyte dysfunction may also be responsible for axonal injury.

Thus, the literature suggests that (1) ALS pathogenesis involves glial cells, inclusion pathology is well documented in oligodendrocytes, and myelination loss is a feature of ALS; (2) oligodendrocytes are heavily dependent on mRNA transport for their function, due to the requirement for *MBP* to be translated in the myelin compartment as opposed to the cell body, where it is toxic; (3) TDP43 is a key component of mRNA transport granules, suggesting that TDP43 pathology may well disrupt oligodendrocyte mRNA transport and thereby myelination; and (4) radiological and pathological studies of animal models and human disease suggest defective myelination in ALS.

We therefore sought to determine the extent of inclusion pathology in human sALS and C9ALS cases and to ascertain whether these inclusions involve oligodendroglia. We investigated how glial inclusion pathology levels in different areas were related. Following this, we assessed myelin integrity. We hypothesised that (1) there would be substantial glial inclusion pathology in both C9ALS and sALS cases; (2) this would affect oligodendrocytes; and (3) there would be disrupted myelin integrity in a manner suggestive of impaired mRNA transport.

Materials and methods

Subjects

Formalin-fixed, paraffin-embedded blocks of precentral gyrus, middle frontal gyrus, and spinal cord from 84 ALS patients with pathologically confirmed disease and 21 controls with no CNS pathology were studied. Of the 84 ALS cases, 66 did not carry any known ALS-causing mutation, and 18 carried a *C9orf72* mutation. Autopsy tissues were donated to the Sheffield Brain Tissue Bank (SBTB) with the consent of the next of kin (supplementary material, Table S1). The SBTB Management Board gave ethical approval for this study under the provision to act as a Research Tissue Bank as approved by the Scotland A Research Ethics Committee (Ref 08/MRE00/103).

Immunohistochemistry

Sections were immunostained using antibodies against p62, carbonic anhydrase II, pTDP43, hnRNPA2/B1, poly-AG, poly-PR, poly-AP, poly-GP, poly-GR, and MAP2+13, an oligodendrocyte precursor cell marker (see supplementary material, Table S2 and refs 24 and 25 for suppliers and methods).

Double-staining immunohistochemistry was performed by first performing immunohistochemistry for the oligodendrocyte marker carbonic anhydrase II (see below) with diaminobenzidene (DAB) as chromogen. This was followed by immunostaining for p62 with tetramethylrhodamine (Alexa Fluor 555). The DAB-labelled oligodendrocytes were visualised in brightfield, while the Alexa Fluor 555-labelled p62 inclusions were visualised by their fluorescence. The two images were then combined to assess co-localisation.

Pathological evaluation

In a single section of spinal cord, the total numbers of p62-positive, pTDP43-positive, and DPR inclusions

were counted, as well as oligodendrocyte precursor cells (OPCs), in the ventral horn and the lateral corticospinal tracts. In the precentral and middle central gyri, inclusions were counted in ten 25× fields and OPCs in 20 25× fields in layer V of the cortex and the underlying white matter. Counting was performed blind using a Dialux 22 brightfield microscope (Leitz, Harlow, UK).

Axonal density in the corticospinal tracts was measured in sections of the cervical spinal cord. For each case, four images of 1280 × 1024 pixels were taken from both tracts (two of each side) using a 100× oil immersion objective. Five stereology-style counting frames were randomly chosen within each image, counting a total of 20 frames from each patient.

The relative number of nuclei labelled for hnRNPA2/B1 in the precentral gyrus white matter and the corticospinal tracts was obtained by counting labelled and unlabelled nuclei in images of these areas taken using a 20× objective.

Post-mortem tissue protein extraction, SDS-PAGE, and western blotting

Tissue was homogenised in RIPA buffer with protease inhibitor (Roche, Welwyn Garden City, UK) and 1 mM 4-benzenesulphonyl fluoride hydrochloride and lysed on ice for 30 min. Extracts were centrifuged at 21 000 × *g* for 5 min at 4 °C, the supernatant was extracted, and a BCA assay (Thermo Fisher, Loughborough, UK) used to measure protein levels. Protein was denatured in 0.125 M Tris–HCl (pH 6.8), 4% sodium dodecyl sulphate, 20% glycerol, 0.2 M dithiothreitol, and 0.02% bromophenol blue at 95 °C for 10 min. Samples (40 µg) were separated by SDS-PAGE and proteins transferred to PVDF membranes. Membranes were blocked in 5% reconstituted cow's milk in Tris-buffered saline with 0.05% Tween 20 for 1 h. Membranes were incubated with primary antibodies (supplementary material, Table S2) at room temperature for 1 h, then with HRP-conjugated anti-mouse or anti-rabbit secondary antibodies for 1 h. Membranes were developed using enhanced chemiluminescence and non-saturated images acquired using a G:BOX EF machine and Snapgene software (Syngene, Cambridge, UK). Protein levels were quantified using GeneTools (Syngene).

Post-mortem tissue RNA extraction, cDNA synthesis, and quantitative PCR

Blocks were dissected from the precentral gyrus white matter and spinal corticospinal tracts and subjected to either Trizol buffer homogenisation or RNA extraction using the Direct-zol MiniPrep Plus kit (Zymo Research, Irvine, CA, USA). cDNA was synthesised from RNA using a SuperScript II Reverse Transcriptase kit (Thermo Fisher) and quantified by qPCR using predesigned 5′ nuclease-quencher assays (Integrated DNA Technologies, Leuven, Belgium) for *MBP* (MBP-001 isoform: RefSeq NM_002385-2, Hs.PT.58.2684380) and *PLP1* (Hs.PT.58.39005119).

Statistical analyses

Normality was tested using the Shapiro–Wilk test and homoscedasticity using the Brown–Forsythe Levene-type test. Stochastic dominance amongst the difference groups was assessed by a Kruskal–Wallis test followed by *post hoc* Mann–Whitney tests where relevant. Correlations were assessed by the Kendall tau rank correlation coefficient.

Results

In the forebrain and spinal cord, the burden of glial inclusion pathology is greater in ALS than in controls and greater in *C9orf72*-ALS than in sporadic ALS

Pathological inclusions affect a minority of cells in ALS, but they are a key pathological feature of disease. We counted the number of neuronal and glial p62-positive ($p62^+$) inclusions in spinal cord (ventral horns and corticospinal tracts), precentral gyrus (cortex and white matter), and middle frontal gyrus (cortex and white matter). No sex difference was found in the inclusion counts ($p \geq 0.1506$).

The pattern that emerged across the grey and white matter of all three regions was that there were greater numbers of $p62^+$ glial inclusions in the ALS cases than in controls, with greater pathology in C9ALS than in sALS cases, and these differences were statistically significant (Kruskal–Wallis test followed by *post hoc* Mann–Whitney FDR < 0.05) (Figure 1; see supplementary material, Table S3 for statistical analyses and supplementary material, Figure S1 for neuronal inclusion counts). Furthermore, the variance in the precentral and middle frontal gyri glial pathology counts was greater in C9ALS than in the control and sALS groups.

We next investigated the relationship between glial pathology levels in adjacent grey and white matter components and between levels of neuronal and glial pathology within structures (Table 1): (1) Levels of glial pathology in adjacent grey and white matter compartments correlated for both sALS and C9ALS cases. (2) There were correlations between the levels of neuronal and glial pathology in the middle frontal and precentral gyri in sporadic cases. C9ALS cases showed fewer correlations. Importantly, correlations between glial pathology levels in the spinal cord and glial pathology in the motor cortex were either low or weak. We conclude that while there is a relationship between the glial pathology load in adjacent grey and white matter compartments, the degree of glial pathology in one structure cannot be inferred from the glial pathology level in a remote structure, even within the motor system.

In sALS brains, glial pathology was more widespread than neuronal pathology: There was glial, but no neuronal, pathology in the grey matter of 22 out of 49 cases in the precentral gyrus and 25 out of 56 cases in the middle

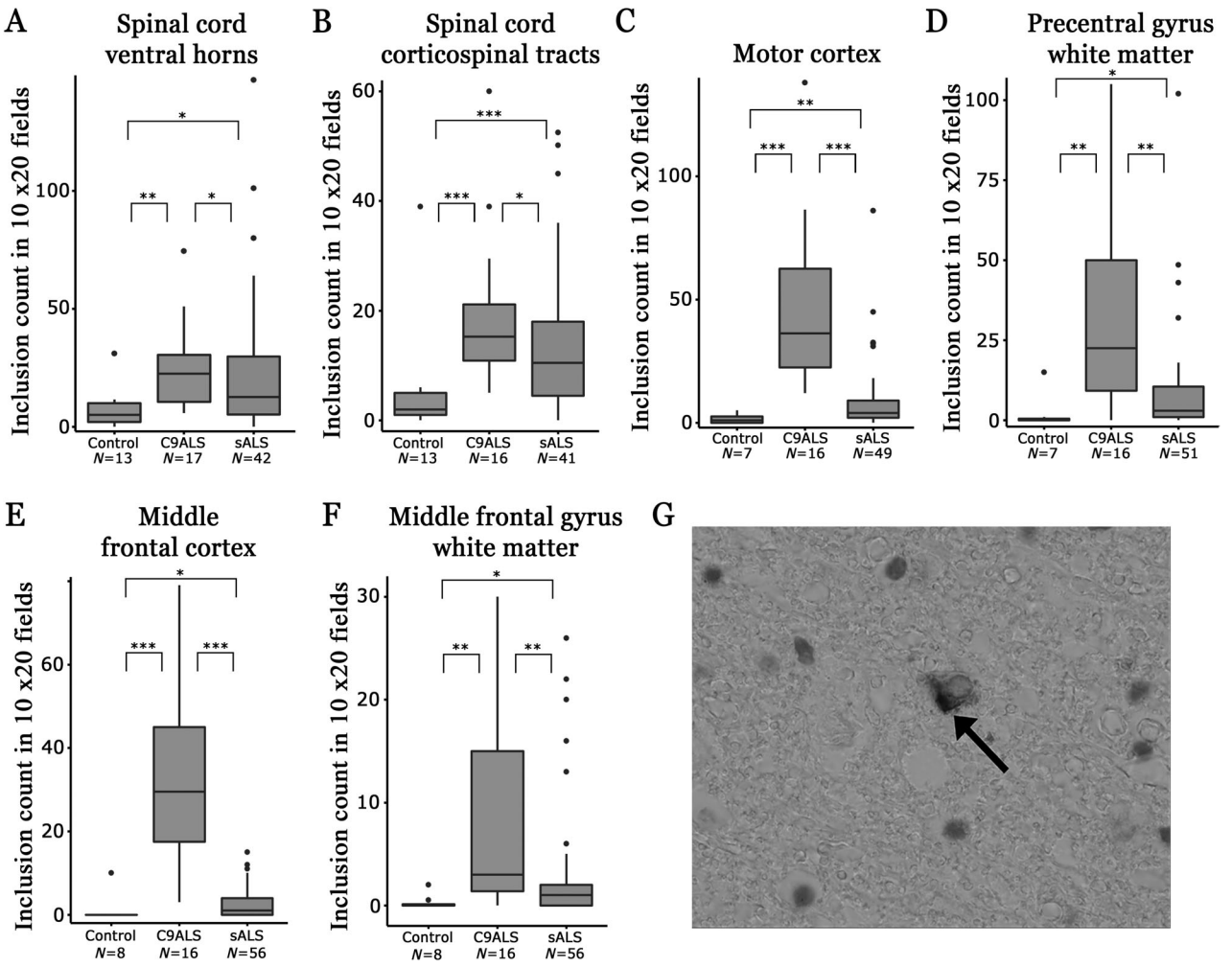

Figure 1. p62$^+$ glial cytoplasmic inclusion body pathology in the brain and spinal cord. Boxplots demonstrate a significantly greater burden of p62$^+$ glial inclusions in sALS cases than in controls, and in C9ALS cases than in both controls and sALS in (A) the grey matter ventral horns, (B) white matter corticospinal tracts, (C, D) precentral gyrus (C, motor cortex; D, underlying white matter), and (E, F) middle frontal gyrus (E, neocortex; F, underlying white matter). *$p < 0.05$, **$p < 0.01$, ***$p < 0.001$. Panel G shows a p62-labelled neuronal cytoplasmic inclusion.

frontal gyrus. This was not the case in C9ALS for which neuronal and glial pathology were present in both brain regions in every case.

We conclude that glial inclusion pathology is a significant burden in ALS. Indeed, it is more widespread than neuronal pathology in sALS brains.

Glial cytoplasmic inclusions are present in oligodendrocytes

The glial cells with p62$^+$ inclusions had morphology that was classically that seen in oligodendrocytes, namely small (approximately 7 μm in diameter) round-to-oval nuclei with compact chromatin. This was confirmed by double-staining immunohistochemistry: Inclusions were demonstrated using p62 and oligodendroglia were labelled with carbonic anhydrase II in the precentral gyrus and spinal cord (supplementary material, Figure S2). Glial cytoplasmic inclusions were present in the small amount of oligodendrocyte cytoplasm adjacent to the nucleus, and often partially or completely encase the nucleus, as can be seen with single-label immunohistochemistry. This obscures it, when visualising the inclusion with DAB. Carbonic anhydrase II was first identified as an oligodendrocyte marker in rats [26] and has been used as such in humans by both us [24] and others [27].

p62$^+$ glial inclusions outnumber pTDP43$^+$ and DPR inclusions combined in C9ALS

In the precentral gyrus, the C9ALS cases showed significantly more p62$^+$ pathology than both controls and sALS cases. We assessed whether these inclusions in C9ALS cases could be explained by either phosphorylated TDP43 or the five possible DPR polypeptides (poly-AP, poly-GP, poly-GR, poly-AG, and poly-PR) as immunolabelled and quantified them using the same protocols as for p62 (Figure 2). The number of glial DPR inclusions was negligible compared with that of p62$^+$ inclusions (all $p \leq 0.0313$). There was a greater number of pTDP43$^+$ inclusions than DPR inclusions, but the burden of this was still lower than that for p62 ($p = 0.0247$). It thus seemed that the DPR and pTDP$^+$

Table 1 Correlations between neuronal and glial pathology in sporadic and *C9orf72*-ALS in various regions by the Kendall tau rank correlation coefficient

Tested variables	*z* value	*P* value	Tau value
C9orf72-ALS			
SC neuronal versus SC glial VH	1.65	0.0988	0.296
SC neuronal versus SC glial CST*	2.35	0.0190	0.437
SC glial VH versus SC glial CST***	3.38	7.25×10^{-4}	0.628
PCG neuronal versus PCG glial cortex	0.0902	0.928	0.0168
PCG neuronal versus PCG glial WM	0.633	0.527	0.119
PCG glial GM versus PCG glial WM*	2.53	0.0115	0.471
MFG neuronal versus MFG glial cortex**	2.89	0.00389	0.538
MFG neuronal versus MFG glial WM	1.55	0.122	0.293
MFG glial GM versus MFG glial WM**	2.99	0.00276	0.564
Sporadic ALS			
SC neuronal versus SC glial VH	1.89	0.0585	0.211
SC neuronal versus SC glial CST	1.89	0.0583	0.215
SC glial GM versus SC glial CST***	6.06	1.34×10^{-9}	0.665
PCG neuronal versus PCG glial cortex***	4.01	5.96×10^{-5}	0.446
PCG neuronal versus PCG glial WM***	3.57	3.56×10^{-4}	0.400
PCG glial GM versus PCG glial WM**	2.71	0.00655	0.282
MFG neuronal versus MFG glial cortex**	3.09	0.00203	0.351
MFG neuronal versus MFG glial WM	0.997	0.319	0.115
MFG glial GM versus MFG glial WM***	3.87	1.11×10^{-4}	0.408

GM, grey matter (cortex or anterior horn); MFG, middle frontal gyrus; PCG, precentral gyrus; SC, spinal cord; WM, white matter (corticospinal tract or white matter in gyrus beneath cortex). *$p < 0.05$, **$p < 0.01$, ***$p < 0.001$.

burden combined was insufficient to explain the burden visualised by p62. In the sALS cases, there was no significant difference between the numbers of inclusions detected by pTDP43 and p62 (Figure 2).

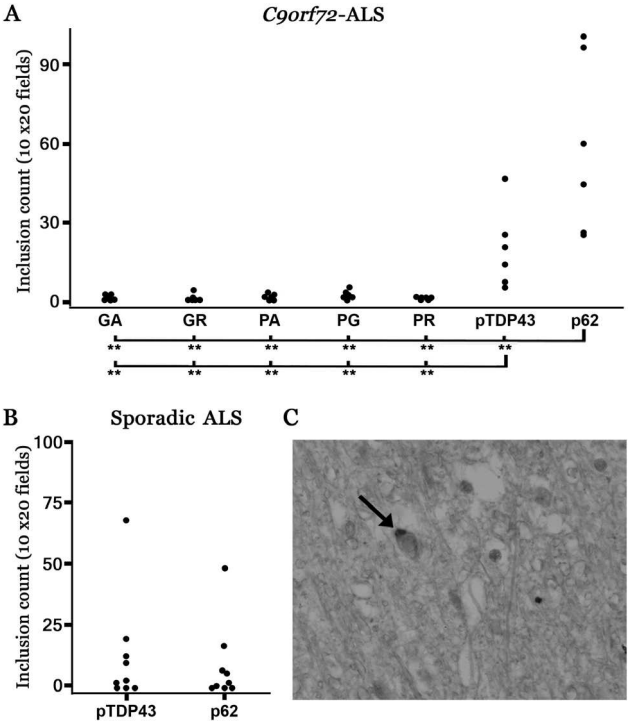

Figure 2. Relative numbers of inclusions that are positive for p62, pTDP43, and five species of RAN-translated DPR. (A) The number of $p62^+$ inclusions vastly outnumber the $pTDP43^+$ and DPR inclusions in the precentral gyrus in C9ALS cases (**$p < 0.01$). (B) There is no significant difference between $p62^+$ and $pTDP43^+$ inclusion counts in sALS cases. Panel C shows a glial poly-AP DPR cytoplasmic inclusion (arrow) in the subcortical white matter of a prefrontal gyrus FFPE section.

The pattern of $TDP43^+$ inclusion pathology reflects the pattern of $p62^+$ in the motor system

We sought to determine whether the pattern of $pTDP43^+$ glial pathology burden was similar to that seen for $p62^+$ pathology in the motor system. Immunohistochemistry for pTDP43 was performed on the spinal cord and precentral gyrus. Glial inclusions that were positive for this antibody were counted in the same manner as for p62 immunohistochemistry above.

Kruskal–Wallis tests found significant intergroup differences in the spinal cord ventral horns and corticospinal tracts, as well as the precentral gyrus white matter and cortex ($p \leq 0.02004$, Figure 3; supplementary material, Table S3 for statistical results). Further *post hoc* analysis revealed that the C9ALS group had greater numbers of $pTDP43^+$ inclusions than controls in the precentral gyrus (motor) cortex and white matter, while the sALS group did not show a significant difference from controls.

In the spinal cord, there were intergroup differences in glial $pTDP43^+$ inclusion scores in the ventral horns ($p = 7.84 \times 10^{-5}$) and the corticospinal tracts ($p = 7.84 \times 10^{-4}$, Figure 3). *Post hoc* tests revealed greater numbers of glial inclusions in both sALS and C9ALS cases than in controls, in common with the pattern seen for p62. There was no significant difference between sALS and C9ALS cases in the inclusion burden.

Myelin pathology in ALS is manifest as a specific deficit in MBP relative to PLP protein levels in the corticospinal tract

Having seen the burden of oligodendroglial $p62^+$ and $pTDP43^+$ inclusion pathology, we predicted that

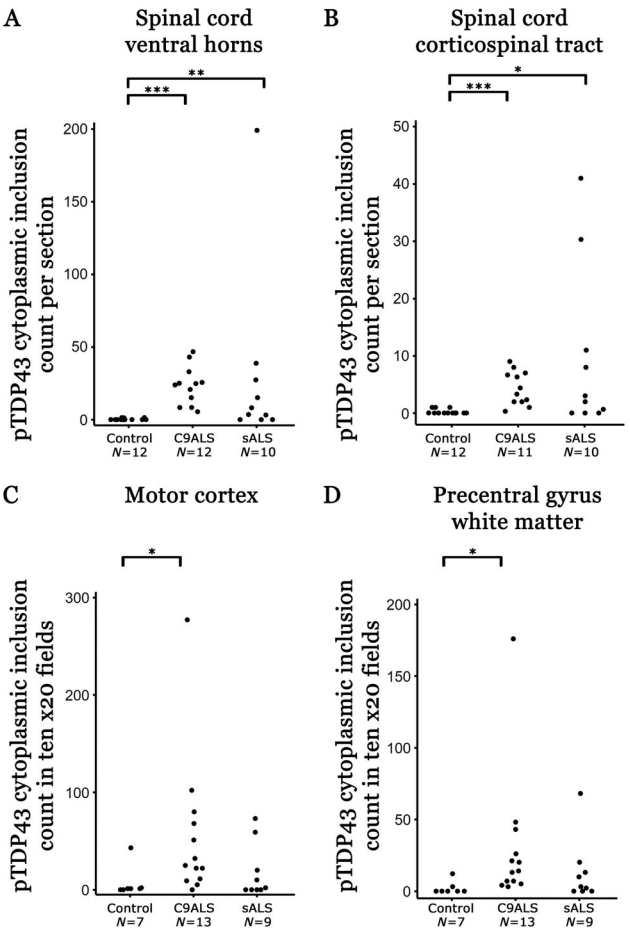

Figure 3. Glial TDP43 pathology. Glial pTDP43$^+$ inclusions are seen in the greatest number in C9ALS cases, in intermediate numbers in sALS cases, and in the lowest numbers in control cases in (A) the ventral horns and (B) corticospinal tracts of the spinal cord. In contrast, glial pTDP43$^+$ inclusion pathology was less marked in (C) the motor cortex and (D) underlying white matter of the precentral gyrus.

oligodendrocytes would also show mRNA transport defects. As described above, myelin basic protein (MBP) is transported as mRNA and then translated to protein. In contrast, proteolipid protein (PLP) is translated in the oligodendrocyte soma and transported as a protein to the myelin compartment. Thus, we hypothesised a disproportionate reduction in MBP compared with PLP protein in ALS corticospinal tract (where pTDP43 pathology is seen in both C9ALS and sALS and shows the greatest contrast between control and ALS groups).

The expression of MBP and PLP protein in the spinal cord corticospinal tract white matter was assessed using western blotting (Figure 4A). The proportion of MBP relative to PLP loss was investigated by normalising MBP to PLP. There were significant intergroup differences in the spinal cord corticospinal tracts. *Post hoc* tests revealed a significant reduction in the levels of MBP normalised to PLP in the spinal cord corticospinal tract in sALS and C9ALS cases compared with controls (Figure 4B). We found no intergroup differences in post-mortem delay ($p = 0.4317$) and no correlation between MBP levels and post-mortem delay ($p \geq 0.48$), and thus conclude that post-mortem degradation cannot explain these results. Furthermore, in the corticospinal tracts, the deficit in MBP in the two ALS groups compared with controls is not significant when MBP is normalised to the internal control, beta-tubulin. Similarly, there are no significant intergroup differences in PLP normalised to beta-tubulin (supplementary material, Figure S3), supporting our contention for a reduction in MBP relative to PLP.

We postulated that the disruption in protein levels of MBP relative to PLP in the spinal cord may be due to mRNA transport defects: Other causes of MBP loss would be more likely to affect both MBP and PLP equally rather than disproportionately affecting MBP. Furthermore, the lack of any intergroup differences in mRNA level implies that the disruption occurred post-transcriptionally. However, we wished to further investigate the possibility of MBP loss occurring secondary to axonal loss in the spinal cord corticospinal tract. We reasoned that if there were a primary defect in MBP, the degree of MBP loss would be out of proportion to the degree of axonal loss. This hypothesis was tested by western blotting for MBP normalised to phosphorylated neurofilament (using SMI31 antibody). Intergroup differences were shown in the MBP/neurofilament ratio in the spinal cord corticospinal tracts ($p = 0.00971$, Figure 4C). In both C9ALS and sALS cases, this ratio was reduced to about 25–50% of that found in controls.

Having identified a deficit in MBP relative to PLP protein in the spinal cord white matter, we set out to determine if this was reflected in a relative deficit in *MBP* relative to *PLP* mRNA. RT-qPCR analysis of spinal cord corticospinal tract mRNA for *MBP* normalised to *PLP* revealed no intergroup differences ($p = 0.484$; Figure 4D).

In contrast to the spinal cord, the precentral gyrus (where there is much less marked p62$^+$ and pTDP43$^+$ pathology in ALS than in controls) showed no differences between groups (Figure 4E,F).

hnRNPA2/B1 expression and the number of oligodendroglial precursor cells correlate negatively with oligodendroglial pathology in the precentral gyrus

The selective reduction of MBP relative to both PLP (another myelin component) and neurofilament (an axonal marker) in the spinal cord raises the possibility of defects in RNA transport. Therefore, we examined the expression of hnRNPA2/B1, a key component of *MBP* mRNA transport granules, in the corticospinal tracts of the spinal cord and in the precentral gyrus white matter by immunohistochemistry: hnRNPA2/B1-positive and -negative glial nuclei were counted to calculate the percentage of glial nuclei that were positive in these areas.

While there were intergroup differences in the percentage of glial cells positive for hnRNPA2/B1 in the spinal cord corticospinal tracts ($p = 0.003$;

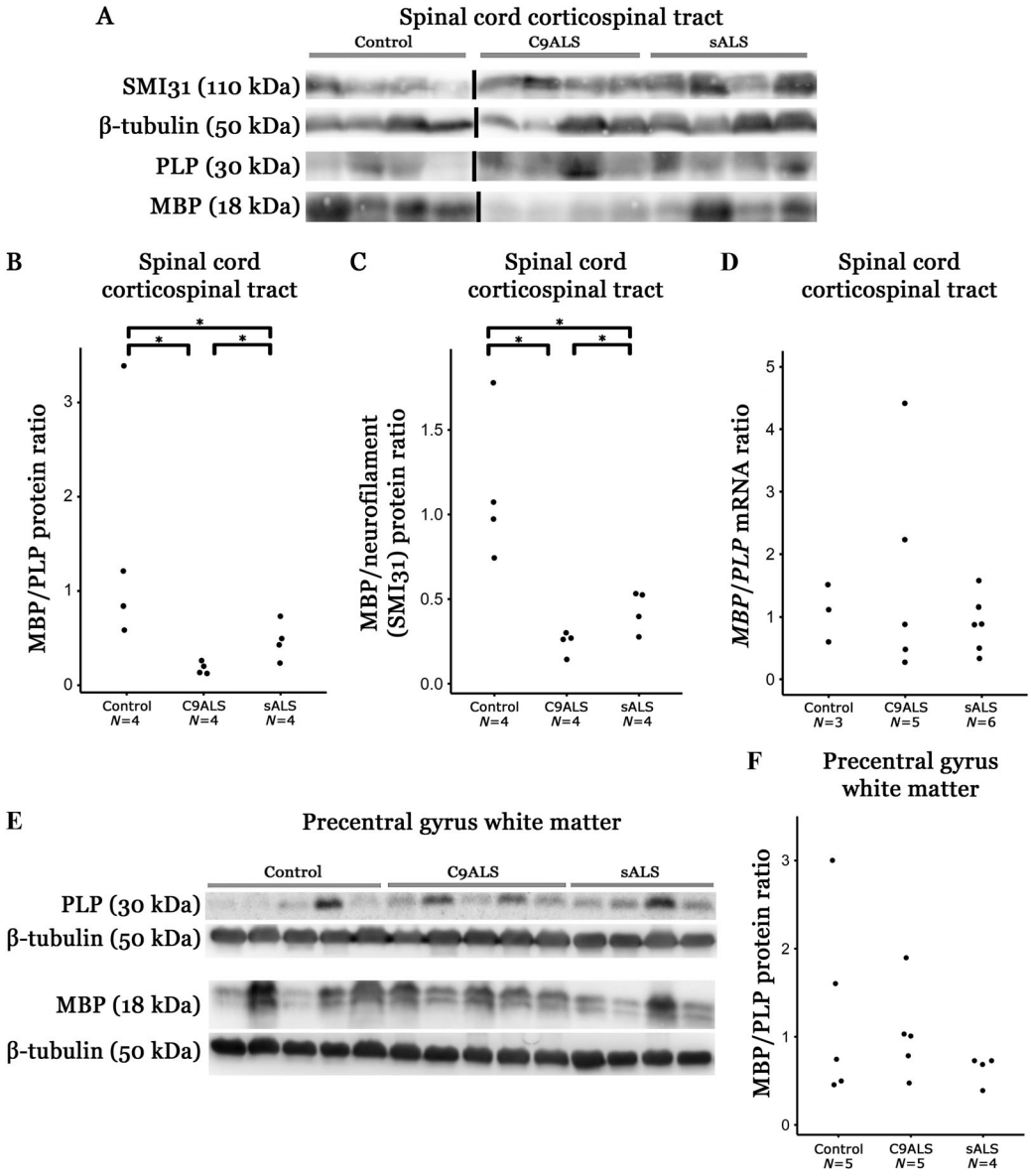

Figure 4. Myelin integrity in the motor cortex and spinal cord. (A, B) In the spinal cord, where the greatest levels of pTDP43^{+} inclusions are seen, immunoblots for myelin components reveal a significant reduction in MBP protein relative to PLP that is most marked in C9ALS cases and intermediate in sALS cases. (C) This MBP reduction is also evident when considered relative to the axonal marker neurofilament. (D) In the spinal cord, the reduction in MBP protein relative to PLP is not reflected in reductions in *MBP* mRNA. (E, F) In the precentral gyrus, where the pTDP43^{+} inclusion burden was less marked, immunoblots of white matter did not reveal a loss of MBP relative to PLP protein.

supplementary material, Figure S4A), *post hoc* analyses revealed these to be due to a difference between C9ALS and sALS cases ($p = 0.003$). There was no significant difference between C9ALS cases and controls ($p = 0.23$), and sALS cases and controls ($p = 0.051$). There were no intergroup differences in the precentral gyrus white matter ($p = 0.741$; supplementary material, Figure S4C). Curiously, the variance seen in the C9ALS group was greater than for the other groups – the same pattern as that seen for the number of p62^{+} and pTDP43^{+} glial inclusions. It was therefore hypothesised that there would be a negative correlation between the percentage of hnRNPA2/B1-positive glia and the burden of glial inclusions in the C9ALS cases in this region. This negative correlation was indeed statistically significant ($p = 0.011$; supplementary material, Figure S4D).

Having shown that glial p62^{+} inclusion pathology loads correlate negatively with hnRNPA2/B1 expression in the white matter of the precentral gyrus in C9ALS cases, it was hypothesised that there would be a commensurate alteration in the numbers of oligodendrocyte precursor cells (OPCs), potentially manifesting as a negative correlation between the number of OPCs and p62^{+} inclusions in the precentral gyrus. OPCs were immunostained (supplementary material, Figure S5F) using the MAP2+13 antibody [28] and counted in the spinal cord ventral horns and dorsolateral spinal tracts (Figure S5A,B), the precentral gyrus grey matter (Figure S5C), and the precentral gyrus white matter (Figure

S5D). As seen with hnRNPA2/B1$^+$ cells, there was a negative correlation between the number of stained OPCs and the number of p62$^+$ inclusions in the precentral gyrus white matter ($p = 0.04$; supplementary material, Figure S5E). There were no significant differences in the number of OPCs between the groups in either the spinal cord or the precentral gyrus.

Discussion

We present post-mortem findings in sporadic amyotrophic lateral sclerosis (sALS) and mutant *C9orf72*-related ALS (C9ALS) cases. First, we quantified p62$^+$ cytoplasmic inclusions in the motor system (spinal cord and precentral gyrus) as well as extra motor tissue (middle frontal gyrus). Consistent with the previous literature, we found that in the motor structures of the spinal cord (ventral horns and corticospinal tracts), there were greater numbers of glial inclusions in both sALS and C9ALS cases compared with controls. Similarly, in the cortex and underlying white matter of the precentral gyrus (motor strip) and middle frontal gyrus (extra motor tissue), both ALS groups (sALS and C9ALS) had greater numbers of glial inclusions than controls. Importantly, a number of sALS cases had glial but no neuronal inclusions in these regions. In contrast to the spinal cord where sALS and C9ALS cases had a similar glial pathology load, in the forebrain, the level of pathology was far greater in C9ALS than in sALS cases and appeared to have a much greater variance in the C9ALS group. The excess of glial pathology in C9ALS compared with sALS is consistent with previous findings [25]. Our first hypothesis that there is a substantial burden of glial pathology in ALS is supported. Double-labelling immunohistochemistry established that the majority of these glial inclusions were in oligodendroglia, supporting our second hypothesis.

Having established the predominance of oligodendrocyte pathology, we aimed to determine the basis for disrupted oligodendrocyte function. To investigate the possibility of a component of myelin disruption being caused by mRNA transport deficiency in oligodendrocytes in the spinal cord corticospinal tracts, we took advantage of the contrasting nature in which the myelin components MBP and PLP are translated and transported: As noted earlier, MBP is transported as mRNA and then translated to protein in the myelin compartment. In contrast, PLP is translated to protein in the cell body and transported to the myelin compartment as protein. Thus, any defect in mRNA rather than protein transport will disproportionately affect MBP compared with PLP. Accordingly, this was demonstrated in our immunoblot assessment of MBP and PLP protein in sALS and C9ALS in the spinal cord corticospinal tract, supporting our hypothesis. There was no significant deficit in MBP in the precentral gyrus, a region with less marked inclusion pathology. Furthermore, the deficit in spinal cord MBP protein was not seen in mRNA level (assessed by RT-qPCR), suggesting that some of the relative MBP protein deficit is caused by mechanisms that act after transcription but before translation, again suggestive of mRNA transport disruption. Furthermore, the MBP loss was out of proportion to the loss of the axonal marker neurofilament protein, suggesting that this component myelin pathology was not secondary to axonal loss. This is not to say that no myelin degradation is secondary to axonal loss, only that axonal loss cannot account for the totality of myelin loss and that primary oligodendrocyte dysfunction is likely to play a part. Some support for this comes from the observation that greater levels of p62$^+$ pathology tended to be seen with lower hnRNPA2/B1 expression in C9ALS.

A limitation of our data on MBP and PLP levels is the inherent inter-individual variability that is a feature of human pathology studies. While the statistical methods employed assess for intergroup differences within the context of inter-individual rank differences rather than variances, this finding of relative reductions in MBP protein in the spinal cord merits replication with a larger series of cases.

Our data are in agreement with Kang *et al*, who found reductions in MBP but not 2′,3′-cyclic-nucleotide 3′-phosphodiesterase (CNPase, another myelin component) in the spinal cords of ALS cases [22]. MBP reductions have also been demonstrated in the G93A *Sod1* transgenic mouse model of ALS [29].

The density of oligodendrocyte precursor cells did not show significant differences between ALS groups and controls in our study. This contrasts with a previous finding of increased NG2 immunoreactivity (which highlights both OPCs and some monocytes) in the post-mortem motor cortex of human ALS cases [22]. Double-staining immunohistochemistry in ALS cases appeared to show a population of hypertrophic Iba1$^-$/NG2$^+$ cells, which were considered to correspond to oligodendroglia. This conclusion should be treated with caution given evidence that some microglia are also negative for Iba1 [30]. Thus, the discrepancy with our study may be due to the differing antibodies used: MAP2+13 tends to target more mature oligodendrocyte precursor cells than NG2 and has less cross-reactivity with monocytes [28].

It is also curious that the C9ALS cases had a p62$^+$ load that was far in excess of the totality of pathology that could be detected by immunohistochemistry for pTDP43 and all five species of dipeptide repeat (DPR). This excessive load of p62$^+$ inclusion pathology in the precentral gyrus of C9ALS cases raises the question of what this antibody is detecting that cannot be quantified by pTDP43 or DPR immunohistochemistry. This is especially true given that the sALS group showed similar levels of inclusions on both pTDP43 and p62 labelling. A number of possibilities exist: First, it is possible that there are DPR aggregates that cannot be detected by the antibodies available to us. Second, it is possible that these p62$^+$ inclusions may also include other proteins that have been found to be incorporated into pathological cellular aggregates in ALS. These

include RNA-binding motif protein 45 [31], Rho guanine nucleotide exchange factor [32], and optineurin [33].

Axonal metabolism is critically dependent on the provision of glucose and lactate by oligodendrocytes [14,34], suggesting that oligodendrocyte function is important for neuronal survival. It is thus possible that oligodendroglial dysfunction could contribute to neuronal death. This has been demonstrated in co-culture systems [9]. Interestingly, recent neuroimaging data demonstrate that white matter degeneration may precede neuronal degeneration in C9ALS, to the point that white matter degeneration may precede symptom onset [35].

In summary, we have observed oligodendrocyte inclusion pathology in brain regions where neuronal pathology was not seen, and a loss of the myelin component MBP that was proportionately greater than the loss of the axon component neurofilament. Together, these observations suggest that oligodendrocyte and myelin pathology can outstrip neuronal pathology in some regions and in a manner that suggests a potential deficit in mRNA transport.

Acknowledgements

We are grateful to the Sheffield Brain Tissue Bank and the very generous individuals who have donated tissue for this research and the next of kin who have accommodated this. This study was largely funded by The Pathological Society of Great Britain & Ireland PhD studentship and a scholarship to ALP for postgraduate studies awarded by 'la Caixa' Foundation (Spain). Some of the work in this project was performed as part of Sampling and biomarker OPtimization and Harmonization In ALS and other motor neuron diseases (SOPHIA), an EU Joint Programme–Neurodegenerative Disease Research (JPND) project funded in the UK by the Medical Research Council. The project is supported through the following funding organisations under the aegis of JPND – https://www.jpnd.eu: France, Agence Nationale de la Recherche; Germany, Bundesministerium für Bildung und Forschung; Ireland, Health Research Board; Italy, Ministero della Salute; The Netherlands, The Netherlands Organisation for Health Research and Development; Poland, Narodowe Centrum Badań i Rozwoju; Portugal, Fundação a Ciência e a Tecnologia; Spain, Ministerio de Ciencia e Innovación; Switzerland, Schweizerischer Nationalfonds zur Förderung der wissenschaftlichen Forschung; Turkey, Tübitak; UK, Medical Research Council. AA and EA were funded by the Deanship of Graduate Studies at King AbdulAziz University. PJS is supported as an NIHR Senior Investigator.

Author contributions statement

ALP, JDW, JK, PJS, and JRH designed the study. ALP, AA, JK, PJS, JDW, and JRH acquired funding. ALP, AH, AA, EA, JK, PJS, JDW, and JRH acquired data and tissues. ALP, AH, JCK, AA, EA, JK, PJS, JDW, and JRH interpreted the data. ALP and JRH drafted the article. ALP, AH, JCK, AA, EA, JK, PJS, JDW, and JRH critically revised the intellectual content. All the authors approved the final version.

References

1. Marin B, Boumediene F, Logroscino G, *et al*. Variation in worldwide incidence of amyotrophic lateral sclerosis: a meta-analysis. *Int J Epidemiol* 2017; **46:** 57–74.
2. McDermott CJ, Shaw PJ. Diagnosis and management of motor neurone disease. *BMJ* 2008; **336:** 658–662.
3. Byrne S, Walsh C, Lynch C, *et al*. Rate of familial amyotrophic lateral sclerosis: a systematic review and meta-analysis. *J Neurol Neurosurg Psychiatry* 2011; **82:** 623–627.
4. Ince PG, Highley JR, Kirby J, *et al*. Molecular pathology and genetic advances in amyotrophic lateral sclerosis: an emerging molecular pathway and the significance of glial pathology. *Acta Neuropathol* 2011; **122:** 657–671.
5. Lagier-Tourenne C, Polymenidou M, Hutt KR, *et al*. Divergent roles of ALS-linked proteins FUS/TLS and TDP-43 intersect in processing long pre-mRNAs. *Nat Neurosci* 2012; **15:** 1488–1497.
6. Brettschneider J, Arai K, Del Tredici K, *et al*. TDP-43 pathology and neuronal loss in amyotrophic lateral sclerosis spinal cord. *Acta Neuropathol* 2014; **128:** 423–437.
7. Philips T, Rothstein JD. Oligodendroglia: metabolic supporters of neurons. *J Clin Invest* 2017; **127:** 3271–3280.
8. Blackburn D, Sargsyan S, Monk PN, *et al*. Astrocyte function and role in motor neuron disease: a future therapeutic target? *Glia* 2009; **57:** 1251–1264.
9. Ferraiuolo L, Meyer K, Sherwood TW, *et al*. Oligodendrocytes contribute to motor neuron death in ALS via SOD1-dependent mechanism. *Proc Natl Acad Sci U S A* 2016; **113:** E6496–E6505.
10. Majounie E, Renton AE, Mok K, *et al*. Frequency of the *C9orf72* hexanucleotide repeat expansion in patients with amyotrophic lateral sclerosis and frontotemporal dementia**:** a cross-sectional study. *Lancet Neurol* 2012; **11:** 323–330.
11. DeJesus-Hernandez M, Mackenzie IR, Boeve BF, *et al*. Expanded GGGGCC hexanucleotide repeat in noncoding region of *C9ORF72* causes chromosome 9p-linked FTD and ALS. *Neuron* 2011; **72:** 245–256.
12. Renton AE, Majounie E, Waite A, *et al*. A hexanucleotide repeat expansion in *C9ORF72* is the cause of chromosome 9p21-linkedALS-FTD. *Neuron* 2011; **72:** 257–268.
13. Cooper-Knock J, Kirby J, Highley R, *et al*. The spectrum of *C9orf72*-mediated neurodegeneration and amyotrophic lateral sclerosis. *Neurotherapeutics* 2015; **12:** 326–339.
14. Lee Y, Morrison BM, Li Y, *et al*. Oligodendroglia metabolically support axons and contribute to neurodegeneration. *Nature* 2012; **487:** 443–448.
15. Aggarwal S, Snaidero N, Pahler G, *et al*. Myelin membrane assembly is driven by a phase transition of myelin basic proteins into a cohesive protein meshwork. *PLoS Biol* 2013; **11:** e1001577.
16. Muller C, Bauer NM, Schafer I, *et al*. Making myelin basic protein – from mRNA transport to localized translation. *Front Cell Neurosci* 2013; **7:** 169.
17. Farg MA, Sundaramoorthy V, Sultana JM, *et al*. C9ORF72, implicated in amytrophic lateral sclerosis and frontotemporal dementia, regulates endosomal trafficking. *Hum Mol Genet* 2014; **23:** 3579–3595.
18. Birsa N, Bentham MP, Fratta P. Cytoplasmic functions of TDP-43 and FUS and their role in ALS. *Semin Cell Dev Biol* 2020; **99:** 193–201.

19. Wang J, Ho WY, Lim K, *et al*. Cell-autonomous requirement of TDP-43, an ALS/FTD signature protein, for oligodendrocyte survival and myelination. *Proc Natl Acad Sci U S A* 2018; **115:** E10941–E10950.
20. Lowe J. New pathological findings in amyotrophic lateral sclerosis. *J Neurol Sci* 1994; **124**(suppl): 38–51.
21. Mollink J, Hiemstra M, Miller KL, *et al*. White matter changes in the perforant path area in patients with amyotrophic lateral sclerosis. *Neuropathol Appl Neurobiol* 2019; **45:** 570–585.
22. Kang SH, Li Y, Fukaya M, *et al*. Degeneration and impaired regeneration of gray matter oligodendrocytes in amyotrophic lateral sclerosis. *Nat Neurosci* 2013; **16:** 571–579.
23. You Y, Joseph C, Wang C, *et al*. Demyelination precedes axonal loss in the transneuronal spread of human neurodegenerative disease. *Brain* 2019; **142:** 426–442.
24. Parkinson N, Ince PG, Smith MO, *et al*. ALS phenotypes with mutations in *CHMP2B* (charged multivesicular body protein 2B). *Neurology* 2006; **67:** 1074–1077.
25. Cooper-Knock J, Hewitt C, Highley JR, *et al*. Clinico-pathological features in amyotrophic lateral sclerosis with expansions in C9ORF72. *Brain* 2012; **135:** 751–764.
26. Ghandour MS, Langley OK, Vincendon G, *et al*. Immunochemical and immunohistochemical study of carbonic anhydrase II in adult rat cerebellum: a marker for oligodendrocytes. *Neuroscience* 1980; **5:** 559–571.
27. Kida E, Palminiello S, Golabek AA, *et al*. Carbonic anhydrase II in the developing and adult human brain. *J Neuropathol Exp Neurol* 2006; **65:** 664–674.
28. Shafit-Zagardo B, Kress Y, Zhao ML, *et al*. A novel microtubule-associatedprotein-2 expressed in oligodendrocytes in multiple sclerosis lesions. *J Neurochem* 1999; **73:** 2531–2537.
29. Niebroj-Dobosz I, Rafalowska J, Fidzianska A, *et al*. Myelin composition of spinal cord in a model of amyotrophic lateral sclerosis (ALS) in $SOD1^{G93A}$ transgenic rats. *Folia Neuropathol* 2007; **45:** 236–241.
30. Waller R, Baxter L, Fillingham DJ, *et al*. Iba-1^{-}/$CD68^{+}$ microglia are a prominent feature of age-associated deep subcortical white matter lesions. *PLoS One* 2019; **14:** e0210888.
31. Collins M, Riascos D, Kovalik T, *et al*. The RNA-binding motif 45 (RBM45) protein accumulates in inclusion bodies in amyotrophic lateral sclerosis (ALS) and frontotemporal lobar degeneration with TDP-43 inclusions (FTLD-TDP) patients. *Acta Neuropathol* 2012; **124:** 717–732.
32. Keller BA, Volkening K, Droppelmann CA, *et al*. Co-aggregation of RNA binding proteins in ALS spinal motor neurons: evidence of a common pathogenic mechanism. *Acta Neuropathol* 2012; **124:** 733–747.
33. Bury JJ, Highley JR, Cooper-Knock J, *et al*. Oligogenic inheritance of optineurin (*OPTN*) and *C9ORF72* mutations in ALS highlights localisation of OPTN in the TDP-43-negative inclusions of *C9ORF72*-ALS. *Neuropathology* 2016; **36:** 125–134.
34. Fünfschilling U, Supplie LM, Mahad D, *et al*. Glycolytic oligodendrocytes maintain myelin and long-term axonal integrity. *Nature* 2012; **485:** 517–521.
35. Querin G, Bede P, El Mendili MM, *et al*. Presymptomatic spinal cord pathology in *c9orf72* mutation carriers: a longitudinal neuroimaging study. *Ann Neurol* 2019; **86:** 158–167.

SUPPLEMENTARY MATERIAL ONLINE

Figure S1. Neuronal $p62^{+}$ cytoplasmic inclusion counts

Figure S2. Glial cytoplasmic inclusions are present in oligodendrocytes

Figure S3. Absolute levels of MBP and PLP in the spinal cord do not differ significantly between control and ALS groups

Figure S4. hnRNPA2/B1 immunohistochemistry in ALS

Figure S5. Counts of MAP2+13 (oligodendrocyte precursor cells)

Table S1. Demographics of cases used for survey of $p62^{+}$ inclusions

Table S2. Sources and conditions for the antibodies used for immunohistochemistry

Table S3. Results of all statistical analyses presented in this paper